The 4th European sCO_2 Conference for Energy Systems
March 23-24, 2021, Online Conference

2021-sCO2.eu-157

OPERATIONAL ANALYSIS OF A SELF-PROPELLING HEAT REMOVAL SYSTEM USING SUPERCRITICAL CO_2 WITH ATHLET

Markus Hofer*
University of Stuttgart
Stuttgart, Germany
Email: hofer@ike.uni-stuttgart.de

Michael Buck
University of Stuttgart
Stuttgart, Germany

Jörg Starflinger
University of Stuttgart
Stuttgart, Germany

ABSTRACT

This study proposes preliminary guidelines for the design and operation of a supercritical carbon-dioxide (sCO_2[1]) heat removal system for nuclear power plants. Based on a thermodynamic optimization the design point is calculated incorporating an existing small-scale compressor map. The behavior of the cycle is tested under varying boundary conditions on the steam side of the compact heat exchanger. The simulations are carried out with the thermal-hydraulic system code ATHLET, which has been extended for the simulation of sCO_2 power cycles. The extensions include the thermodynamic properties, heat transfer and pressure drop correlations as well as performance map based turbomachinery models, which take the real gas behavior of sCO_2 into account. During the decay heat transient, compressor surge occurs in some of the simulated cases. In order to avoid compressor surge and to follow the decay heat curve, the compressor speed is reduced together with the steam temperature. This enables to operate one single system down to a thermal load of less than 50 % even under the design restriction caused by the application of the existing compressor performance map.

INTRODUCTION

In case of a station blackout (SBO) and loss of ultimate heat sink (LUHS) accident in a boiling water reactor (BWR) or pressurized water reactor (PWR), the plant accident management strongly depends on the depends on the recovery of electricity, e.g. by emergency diesel generators, or from external sources. If not available, core integrity may be violated, like in Fukushima Dachii. Such scenarios lead to the development of advanced decay heat removal systems. Since space is a limitation in existing power plants, the supercritical carbon-dioxide (sCO_2) heat removal system "sCO2-HeRo" was proposed [1–3]. This system can be incorporated in new nuclear power plants as well as retrofitted to existing nuclear power plants. The system consists of a compact heat exchanger (CHX), a gas cooler, serving as the ultimate heat sink (UHS), and the turbomachinery, one compressor and one turbine mounted on a common shaft together with a generator. Since the momentum from the turbine is sufficient to simultaneously drive the compressor and generate more electricity than used by the fans of the UHS, the system is self-propelling. The excess electricity can even be used to support other accident measures, e.g. recharging batteries. sCO_2 is selected as a working fluid because of its favorable fluid properties, enabling the design of a very compact system. Moreover, sCO_2 is not combustible, non-toxic and commercially available.

Figure 1 shows the scheme of the sCO2-HeRo attached to a BWR. In the case of an accident the valves, which connect the compact heat exchanger (CHX) to the main steam line, open automatically. Driven by natural circulation, the steam condenses and heats the sCO_2 in the CHX. Due to the space limitations, the CHX consists of many channels with a small hydraulic diameter, so called mini-channels, in order to reach a large heat transfer area [1]. The pressurized and heated sCO_2 is expanded in the turbine, which drives the compressor and generates power for the fans of the gas cooler. After the turbine, the remaining heat of the sCO_2 is removed in the gas cooler to the ultimate heat sink. Finally, the sCO_2 is compressed and flows to the CHX. Similarly, the sCO2-HeRo can be attached to the

[1] sCO_2 is defined as carbon dioxide at supercritical conditions with $p > 73.8$ bar and $T > 31$ °C

* corresponding author(s)

DOI: 10.17185/duepublico/73983

secondary loop of a PWR. In the primary loop natural circulation will develop due to the decay heat input and the heat removal via the steam generator. Consequently, the sCO2-HeRo can be used for BWRs as well as PWRs.

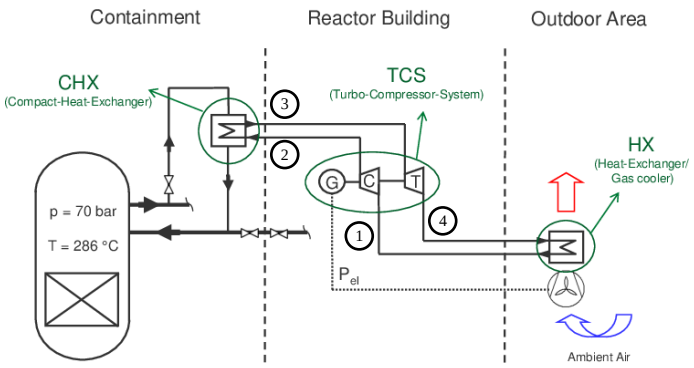

Figure 1: The sCO_2 heat removal system attached to a BWR [1] including the different states in the cycle: compressor inlet (1), compressor outlet (2), turbine inlet (3), turbine outlet (4)

For the simulation of nuclear power plants, different thermal hydraulic system codes are used, e.g. CATHARE, RELAP, TRACE and ATHLET [4]. Because sCO_2 is also considered as a working fluid in the power generation cycle of 4th generation reactor concepts, work is in progress to extend these system codes for the simulation of sCO_2 power cycles [1], [5], [6], [7], [8]. Venker investigated the feasibility of the sCO2-HeRo approach for a BWR in detail and implemented first extensions in ATHLET for the simulation of the heat removal system. First simulations showed that the grace period can be extended to more than 72 h [1]. The grace period is the period of time for which the nuclear power plant remains in a safe condition without the need of human interaction [9]. In the frame of the sCO2-HeRo-project further reports and studies were published, e.g. dealing with the start-up of the system or the design and control [2,10–12]. In the frame of the project, Hecker and Seewald [10] analysed the decay heat removal from a BWR with a nuclear power plant simulator. This analysis suggested that manual actions by operators and a higher heat removal capacity than proposed by Venker would be necessary to avoid automatic depressurisation at low level in the reactor vessel. Because a comparable level drop on the secondary side of a steam generator does not initiate automatic depressurization from the reactor protection system, more operational flexibility can be expected for a PWR. Hajek et al. describe the basic principles for the integration of the sCO2-HeRo into the European PWR fleet including safety, reliability and thermodynamic design considerations [11,12]. Hofer et al. carried out preliminary design calculations and provided considerations for the operation of the Brayton cycle, e.g. it may be beneficial to locate the design point of the turbomachinery in part load and the system may be operated via a shaft speed control [13].

In general, the analysis of the sCO2-HeRo approach can be conducted considering different time intervals and levels of complexity. In terms of time, the accident can be divided into the first phase, where the decay heat exceeds the heat removal capacity of the system, and the second phase, where the heat removal capacity is higher. Regarding complexity, different parts of the system or the whole system can be analyzed. This paper focusses on the sCO_2 cycle including the steam side of the CHX and on the second phase regarding time. Compared to previous publications, the sCO_2 cycle is modelled and analyzed in more detail. In the theoretical section, this paper shortly presents design and operational considerations for the sCO2-HeRo system and the extensions of the thermal-hydraulic system code ATHLET (Analysis of THermal-hydraulics of LEaks and Transients). In the results section, the system design is provided using the scaled performance map of the compressor designed in the sCO2-HeRo project [8,14]. Afterwards, the system is simulated in ATHLET considering and comparing different control strategies.

THEORY

Cycle design and operation

In case of an accident, the main purpose of the sCO2-HeRo system is to remove the decay heat reliably over several days. Due to the exponential decrease of the decay heat and due to changing ambient conditions, the system must be able to operate over a wide range of conditions. From a thermodynamic point of view, the worst condition for the system occurs at the highest ambient temperature and the smallest decay heat input per system, which is considered. Consequently, it might be a valid approach to start the system design from this point. However, the lowest ambient temperatures must also be taken into account, because if no operational action is undertaken the compressor inlet temperature will decrease with the ambient temperature. This leads to an increasing compressor inlet density and potentially drives the compressor to surge. To avoid approaching the surge line, one option is to keep the compressor inlet temperature sufficiently high. This can be achieved by decreasing the fan speed in order to decrease the performance of the gas cooler. However, it must be checked if this measure is sufficient for the lowest ambient temperatures because heat transfer occurs also with the fans switched off. An additional measure is to design a modularized gas cooler which enables decoupling of certain sections or to increase the compressor mass flow rate via a bypass. Ambient temperature variations and extremely low ambient temperatures are not in the scope of this paper and will be analyzed in the future. This paper analyses the operation of the system at the highest ambient temperature, which is assumed to be 45 °C, with the naturally declining decay heat as boundary condition.

The next step to the system design is to define the maximum thermal power, which must be removed reliably by the system. Venker has shown that it is not necessary to design the system for the maximum decay heat occurring directly after the reactor scram [1]. Depending on the power plant type (BWR or PWR), the time delay allowed to start the system along with additional supporting systems, as well as the required system capacity differ. As a first step, the required system size can be determined

with a simple heat balance or obtained by means of reactor simulations where the system is represented by a heat sink. As long as the decay power exceeds the thermal power of the system, steam is blown off to keep the pressure below a certain threshold. Since, it is assumed that the water inventory cannot be replaced, the water level must be kept high enough to enable the operation of the sCO2-HeRo as well as to ensure the cooling of the reactor core. Former analysis demonstrated that more than one system is needed to follow the declining decay heat curve [1]. In this paper, a system size of 10 MW is selected, which enables the use of this system for different reactor types and sizes, because just the number of systems has to be adapted. A simple heat balance suggested that 60 MW might be sufficient for a PWR with a thermal power of 3840 MW. Comparing the total power of the sCO2-HeRo system to the decay heat curve suggests a power break even after 3000 s. Thus, the system operates at its maximum power from start-up to 3000 s and then the system has to adapt to the declining decay heat, shown in Figure 2. According to the User Manual of ATHLET ANS Standard ANS-5.1-1979 is used [15] and the same curve as in the analysis of Venker is applied, which is the decay heat occurring after 300 days of operation [1]. After the power break even, removing more power from the reactor than is produced by the decay heat will cause a cool down of the reactor. This results also in a lower temperature difference being available for the sCO2-HeRo and eventually will stop the operation of the system because the power balance becomes negative as will be shown in the results section. Venker already demonstrated the need for a balance between heat generation and heat removal in order to obtain a stable operation of the sCO2-cycle attached to a BWR [1]. Since the decay heat is decreasing continuously, it might be necessary to control the system in part load. The required part load capability of the system also depends on the number of systems installed and the control strategy. Future analysis will consider these aspects in more detail. However, the general procedure and the conclusion presented in this paper will still stay valid because this analysis is not dependent on the system size or the time of power break even.

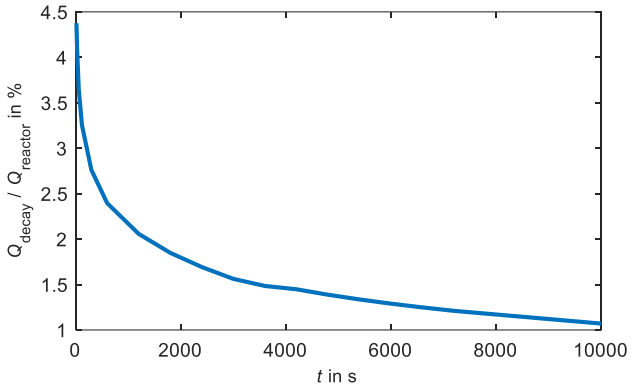

Figure 2: Decay power [1,10,15] divided by the thermal power of the reactor over time

After these general considerations the thermodynamic design of the system will be discussed in more detail. As mentioned before, the worst operation point of the system is the lowest power input per system at the highest ambient temperature. At this point, the turbomachinery efficiencies must be high enough to guarantee a self-propelling operation. This should be considered in future designs using an integrated design approach, which iteratively adapts the cycle and turbomachinery design. In this paper, the design will be carried out at the maximum power input per system with an existing compressor performance map. The heat exchangers should also be designed for this point because they are required to remove the design power. The thermodynamic cycle design can be conducted using a simple thermodynamic optimization [13] using the basic thermodynamic relations for and between the components also involving the isentropic efficiencies of the compressor and the turbine [16]. The optimization maximizes the specific power output of the system and not the efficiency because the system shall be self-propelling as long as possible and the system efficiency is of no interest. For given compressor inlet temperature ϑ_1, turbine inlet temperature ϑ_3, turbomachinery efficiencies η_c and η_t, pressure drops in the heat exchangers Δp_{UHS} and Δp_{CHX} and the relative power consumption of the fans k_{fan}, the compressor inlet and outlet pressure p_1 and p_2 are optimized to maximize the specific power output of the system

$$\Delta w = f(p_1, p_2, \vartheta_1, \vartheta_3, \eta_c, \eta_t, k_{fan}, \Delta p_{UHS}, \Delta p_{CHX}). \quad (1)$$

For the thermodynamic design point optimization, the piping pressure drop is neglected and the power of the fans is assumed to be a linear function of the heat removal capacity. The excess power of the cycle ΔP is calculated by multiplying Δw with the mass flow rate of the cycle.

Simulation of the Brayton cycle

The code extensions of ATHLET described in the following can be found in more detail in publications of Venker [1] and Hofer et al. [8,17]. In the supercritical region, the thermodynamic properties of CO_2 are calculated with fast splines, which were derived from the equation of state [18]. In ATHLET, the heat transfer coefficient of CO_2 is calculated with the Gnielinski correlation [19]. The pressure drop of supercritical CO_2 is derived from the Colebrook equation, which is recommended for normal pipes as well as for mini-channels [20]. Additionally, form loss coefficients can be applied, to e.g. model the inlet and outlet plenum of the CHX. For water the implemented correlations [21] are used except for the film condensation, where the ATHLET correlations were improved [17] and now the correlations given in [22,23] are used. For turbine and compressor, different models are available. In this paper, Stodolas cone law [24] and an efficiency correlation for radial turbines [25] is used for the turbine. The compressor is simulated with a performance map approach [8,26]. The performance map generated from experimental data or CFD simulations is transposed to a dimensionless map, shown in Figure 3.

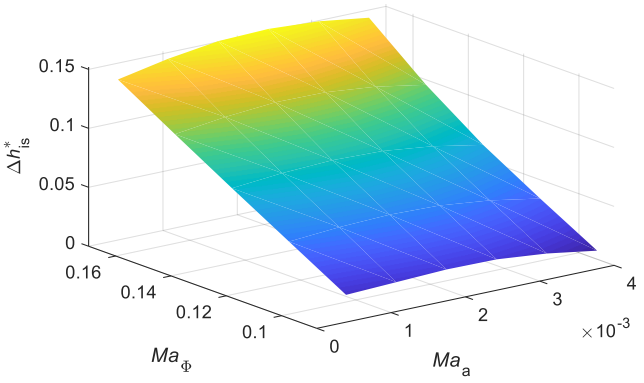

Figure 3: Dimensionless isentropic enthalpy difference $\Delta h_{is}{}^*$ as a function of the axial and tangential Mach Numbers (Ma_a and Ma_θ)

The x- and y-axis are the axial and tangential Mach numbers, given by

$$Ma_a = \frac{\dot{m}}{\rho c D^2} \quad (2)$$

$$Ma_\theta = \frac{ND}{c}, \quad (3)$$

where N is the rotational speed, D the impeller diameter and c the speed of sound. All thermodynamic parameters are determined for the inlet condition. As main difference to other performance map approaches, the speed of sound is calculated via the equation of state and not using ideal gas assumptions. On the z-axis the dimensionless isentropic enthalpy difference $\Delta h_{is}{}^*$ or the corrected pressure ratio π_c and the efficiency η can be presented. The equation for the dimensionless isentropic enthalpy difference is

$$\Delta h_{is}{}^* = \frac{\Delta h_{is}}{c^2}. \quad (4)$$

RESULTS AND DISCUSSION

Cycle design

As mentioned in the theory section, the cycle design is carried out for the maximum heat load, which is 10 MW per unit, at an ambient temperature of 45 °C. The boundary conditions for the design calculation are summarized in Table 1. With the pinch point temperature differences, the compressor and turbine inlet temperature can be calculated. Then the optimal design point can be found according to the procedure described in the theory section. However, for the simulation of the compressor an existing performance map of small-scale compressor [14] shall be scaled-up and used. This is carried out using equations 2, 3 and 4 and, but conservatively, without any additionally efficiency correction. Therefore, the efficiency of the large-scale compressor is equal to the efficiency of the given small-scale compressor. The pressure ratio and the outlet state can be determined with the inlet state and the performance map using equation 4. Since, the condition at the compressor inlet is also given by the thermodynamic optimization, the compressor outlet condition is defined by the underlying performance map. Thus, the optimization of p_1 and p_2 reduces to an optimization of only p_1 with p_2 given by the compressor characteristic.

Table 1: Boundary conditions for the design process

Parameter	Unit	Value
$\dot{Q}_{CHX}$	MW	10
$\Delta T_{PP,CHX}$	K	10
$\Delta T_{PP,UHS}$	K	5
$\Delta T_{sub,H2O}$	K	8
Δp_{CHX}	bar	2
Δp_{UHS}	bar	0.25
$\vartheta_{in,H2O}$	°C	296
$h_{in,H2O}$	kJ/kg	2760
η_c	-	0.72
η_t	-	0.8
k_{fan}	kW_{el} / MW_{th}	8.5

The thermodynamic design parameters from the optimization process are summarized in Table 2. Compared to conventional sCO_2 cycles, the design point is located quite far above the critical point with a compressor inlet state of 50 °C and 12 MPa. The high compressor inlet pressure results from the high design point ambient temperature of the system.

Table 2: Optimal thermodynamic design point with the restriction of the existing compressor performance map

	ϑ in °C	p in MPa
Compressor Inlet (1)	50	12
Compressor Outlet (2)	69	18.8
Turbine Inlet (3)	286	18.7
Turbine Outlet (4)	246	12

In Figure 4, the power output for the optimized design conditions is shown varying the turbine inlet temperature and the pressure ratio. The actual design point is located at the maximum temperature and at a pressure ratio of 1.57. On the contrary, the theoretical optimal design point is also located at the maximum temperature and at a pressure ratio of 3.09. The power output of the system at these two points is 440 kW and 807 kW,

respectively. Due to the application of an existing small-scale compressor map, the thermodynamic design point deviates from the optimal design point in terms of pressure ratio. The efficiency of the system with 4.4 % is quite small. However, as mentioned before, the only task of the system is to remove the decay heat reliably and not to generate power, therefore, the efficiency is of no interest. The lower pressure ratio of the actual design might result in a worse performance in the transient calculation because e.g. reducing the shaft speed decreases the pressure ratio further. However, the main focus here is to present the procedure and to enable an off-design simulation of the system and not to give quantitative results for the best system design. Additionally, it might be sufficient to choose a compressor with a pressure ratio smaller than the optimum value, which might reduce the system cost keeping in mind that the pressure ratio of a single stage compressor is technically limited to approximately 2.0. The compressor speed and the impeller diameter of the large-scale compressor can be determined using equations 2 and 3. Since, the design point Mach numbers of the small-scale machine are the same for the large-scale machine and the compressor inlet condition is given by the thermodynamic optimization, it is possible to solve the two equations for the two unknowns. This results in a compressor impeller diameter of 0.22 m and a rotational speed of 12700 1/min.

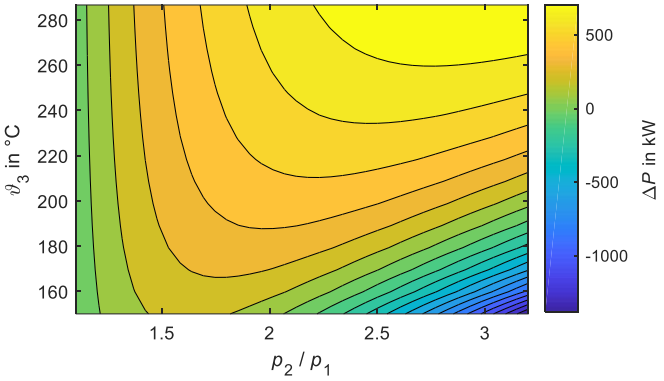

Figure 4: Maximized power output ΔP as a function of pressure ratio p_2/p_1 and turbine inlet temperature ϑ_3 for the given design boundary conditions

The geometry of the CHX plates follows [16,17]. The channel length and number are adapted to reach the desired temperatures and transferred power. The steam is assumed to enter the CHX saturated and to leave slightly subcooled. For the 2x1 mm rectangular channels, this results in 11070 channels with a length of 0.85 m. They can be arranged into 90 plates with 123 channels each, leading to a size of approximately 0.9 m x 0.4 m x 0.2 m. For the UHS an existing design [27] was scaled down leading to 190 pipes with a length of 15 m. For simplicity the design only covers the sCO_2-side. The pipe length between the components and the diameter is assumed to 22.5 m and 0.2 m, respectively [12]. The whole design is valid for a cycle attached to a PWR. In case of a BWR the steam temperature could be slightly lower due to the lower blow-off pressure. This can be compensated by slightly modifying the whole design or by just adapting the CHX to reach a lower pinch point temperature difference.

Simulation of the Brayton cycle

In this section, the simulated system, the boundary conditions and the simulation results for the sCO2-HeRo cycle are shown and operational conclusions are drawn. Assuming that in the first phase of the accident the heat removal system operates at its maximum capacity of 10 MW per unit, the transient analysis is started at 3000 s when the decay power is equal to the system capacity. As mentioned before, the ambient temperature is set to 45 °C. However, this is not modelled explicitly, because no design of the air-side of the UHS is available. Instead, it is assumed that the cooling power $\dot{Q}_{UHS}$ can be controlled via the fan speed to reach the desired temperature difference between the compressor inlet temperature $\Delta T_{PP,UHS}$ and the ambient temperature. This assumption should be valid because the decay power is declining slowly after 3000 s. Since the nuclear power plant is not simulated, boundary conditions for the steam must be provided. The conditions at the start are given by the design with saturated steam at 296 °C at the inlet and slightly subcooled water at 288 °C at the outlet of the CHX. From a power balance, the steam mass flow rate can be determined, which is 7 kg/s at the design point of the system. The initial conditions are the same for all cases. During the transient, the enthalpy at the inlet of the CHX are always kept at the saturation point of steam for the given temperature. Therefore, the pressure at the inlet is also the saturation pressure. To provide an overview of the boundary conditions, they are summarized in Table 3 and the case specific boundary conditions will be explained in detail at the beginning of each case.

Table 3: Boundary conditions of analyzed cases

	Case 1	**Case 2**	**Case 3a**	**Case 3b**	**Case 4**
$\dot{m}_{H2O}$	declining	constant	declining	declining	calculated
$h_{in,H2O}$	at saturation point of steam (x=1) for all cases				
$\vartheta_{in,H2O}$	constant	declining	constant	constant	declining
$\Delta T_{sub,H2O}$	not constant (result)		constant at design value		
$\Delta T_{PP,UHS}$	constant at design value except for 3b (increasing)				
N	constant at design value		controlled to match $\Delta T_{sub,H2O}$		
$\dot{Q}_{UHS}$	controlled to match $\Delta T_{PP,UHS}$				
$\dot{Q}_{CHX}$ / $\dot{Q}_{decay}$ (result)	>1	≈1	1		

The nodalization of the ATHLET model is shown in Figure 5. The H_2O side consists of an inlet, an outlet and the CHX channels. The enthalpy is specified at the inlet and the pressure at the outlet. Through a heat conduction object the H_2O side is

connected to the CO_2 side. The CO_2 side is a complete cycle with four pipes connecting the components, namely the compressor, the CHX, the turbine and the UHS. The compressor and the turbine component are described by lumped parameter models providing sink or source terms for the momentum and energy conservation equation [8]. The CHX is modelled with a representative channel pair including form loss coefficients for the inlet and outlet plenum [8,17]. As mentioned before, the heat transfer in the UHS is not modelled explicitly. Instead, the power input to the UHS is adapted, to match a certain compressor inlet temperature.

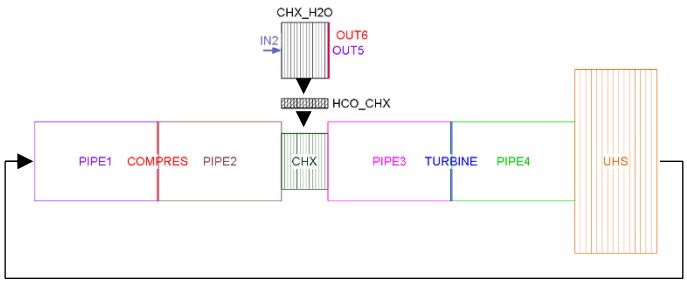

Figure 5: Nodalization of the ATHLET model

Case 1

In a first simulation, the system is operated at its design speed. The steam mass flow rate $\dot{m}_{H2O}$ is defined to follow the decay heat curve, which means if inlet and outlet conditions stayed constant at their design values given in Table 1, the transferred power would exactly equal the decay power. However, in off-design the transferred power is higher than the decay power, as shown in Figure 6, because the condensate is subcooled compared to the design point. Thermodynamically, this would lead to a decreasing steam temperature as well as steam pressure because of the negative thermal power balance. Therefore, the inlet conditions of the CHX would change in reality, which affects the performance of the system. This is analysed in case 2.

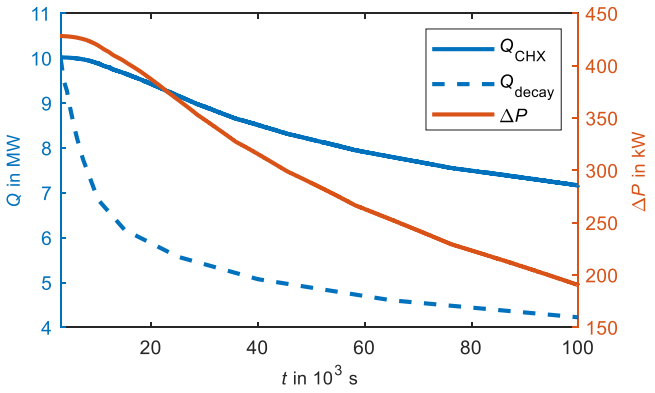

Figure 6: Decay power $\dot{Q}_{decay}$, removed power $\dot{Q}_{CHX}$ and power output of the system ΔP over time for case 1

For completeness, Figure 6 also includes the power output of the system. However, this value has to be interpreted with care because the thermodynamic conditions in a real power plant will change as explained before. Another important point about this simulation is the operation of the compressor. It can be observed that the compressor operates at higher Ma_a and Ma_θ than in the design. This is caused by the decrease of the compressor inlet pressure at an almost constant mass flow rate. Since, the performance map ends at the design Ma_θ, the results of this simulation must be interpreted carefully because either the performance calculated by linear extrapolation might be unrealistic or the compressor might even not be able to work in this region anymore. At the time, when the simulation stops, Ma_θ is 9 % higher than its design value. Therefore, if the system shall be operated at constant speed all the time, it is necessary to extend the performance map and it might be required to design the compressor and the shaft for higher loads.

Case 2

In a second simulation, the shaft speed of the turbomachinery is kept constant again. The effect of the cool down of the steam side is examined. The steam mass flow rate is kept constant at its design point and the steam inlet temperature and pressure are decreased keeping the inlet saturated. The decrease is adapted to approximately follow the decay heat curve, which can be observed from Figure 7. This enables to analyse the influence of decreasing steam temperatures on the sCO_2 cycle. In the nuclear power plant, the steam temperature would decrease with some delay because of the large water inventory. In this case, the sCO_2 cycle stops operating at a steam temperature of 175 °C at 25000 s, because the power balance becomes negative, which is shown in Figure 7.

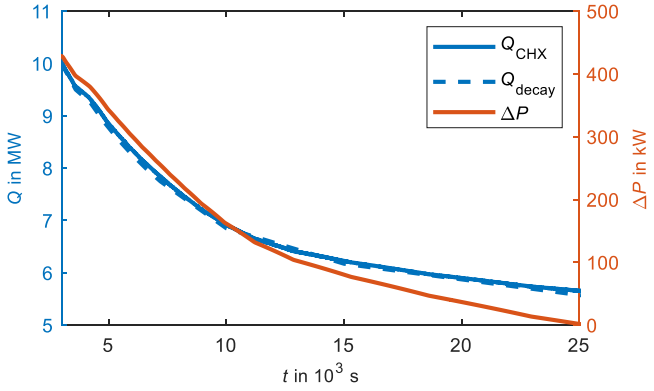

Figure 7: Decay power $\dot{Q}_{decay}$, removed power $\dot{Q}_{CHX}$ and power output of the system ΔP over time for case 2

The negative influence of decreasing steam temperatures and, therefore, turbine inlet temperatures can be also observed from Figure 4. A failure of all sCO2-HeRo systems can be avoided by either switching off single units at the right time, as suggested by Venker [1], or by controlling the transferred power of the systems or by a combination of both measures. The

disadvantage of just switching off single units at a certain time is that the right time for the shutdown needs to be determined. Another option would be to follow the decay heat curve by controlling the sCO_2 cycle. This will be analysed in the next case.

Like in the previous case, it has to be noted that the compressor operates at higher Ma_a and Ma_θ than in the design. This is due to the same reasons as in case 1. At the time, when the simulation stops, Ma_θ is 14 % higher than its design value. In this case, the effect is stronger because the compressor inlet pressure decreases further.

Case 3

In the third simulation, the boundary conditions of the first simulation are applied and, additionally, the shaft speed of the turbomachinery is controlled in order to keep the sub-cooling $\Delta T_{sub,H2O}$ at the water outlet constant. Thus, all thermodynamic conditions of the water-side remain constant, only the mass flow rate varies according to the decay heat. Therefore, the removed heat exactly equals the decay heat. At the beginning, this method works well, but after 20000 s the system stops because of compressor surge. The operation line of the compressor is shown in Figure 8 together with the numerical surge line. The current case is labelled "3a". The numerical surge line is located where Δh_{is}^* reaches its maximum with changing Ma_a. To the right of the surge line is the stable operation range, to the left of it the unstable range. The other simulations also included in this figure are presented in the following sections. Additionally, the cycle mass flow rate over time is displayed in Figure 8 to indicate the stop of the system and support the following discussion.

When the compressor crosses the surge line in the simulation, the simulation becomes unstable and stops. In order to avoid compressor surge, the decrease of the axial Mach number Ma_a must be limited. According to equation 2, this can be achieved by reducing the density and the speed of sound at the compressor inlet (measure 1) or by limiting the mass flow rate decrease compared to the current simulation (measure 2). Measure 2 can be enforced by decreasing the steam temperature, as explained later together with case 4, or with a compressor recirculation line or a turbine bypass. In this paper, only the basic layout without additional bypasses is considered to keep the heat removal system as simple as possible. Furthermore, since no inventory control system has been considered, measure 1 can only be achieved by increasing the compressor inlet temperature ϑ_1 (measure 1.1) or by decreasing the inlet pressure p_1 (measure 1.2). An increase of ϑ_1 can be achieved by also increasing the temperature difference between the ambient air and the compressor inlet $\Delta T_{PP,UHS}$. This action corresponds to a decrease of the fan speed.

In simulation 3b, this measure is tested by applying all boundary conditions of simulation 3a except for $\Delta T_{PP,UHS}$, which is increased steadily during the simulation. From Figure 8, it can be observed that the compressor surge is postponed but still occurs after 45000 s. At this time, ϑ_1 is already increased by 13 K and the power output of the system almost decreased to zero. Thus, the increase of ϑ_1 also leads to a lower power output of the system. Consequently, the system will stop due to either compressor surge or a negative power balance. The occurring compressor surge is mainly due to the decrease of the mass flow rate, which is similar to simulation 3a. Therefore, measure 1.1 is not sufficient without taking into account measure 2. Furthermore, measure 1.1 should be avoided due to the negative impact on the power output, as explained above.

Case 4

In order to define the boundary conditions for the next simulation, it is necessary to understand how the compressor inlet pressure (measure 1.2) and the mass flow rate of the cycle (measure 2) can be influenced. At a constant power input the cycle mass flow rate increases when the enthalpy difference of the sCO_2 over the CHX decreases. The current enthalpy difference is mainly linked to the steam temperature and decreases as the steam temperature decreases. A reduction of the steam temperature also reduces the temperatures at the hot side of the sCO_2 cycle and, therefore, increases the density. Due to constant mass inventory in the cycle, a part of the mass from the cold side moves to the hot side of the cycle and, therefore, pressure and density at the compressor inlet decrease. Thus, both measure 1.2 and measure 2 can be achieved by decreasing the steam temperature.

Therefore, simulation 4 investigates a steam temperature decrease. At the foreseen end of the simulation at 100000 s, the steam temperature is arbitrarily reduced to 200 °C and the temperature decrease is assumed to follow the decay heat curve. Like in the previous simulations, the enthalpy and pressure at the inlet are set to saturation conditions. It is assumed that the mass flow rate of the steam changes with the decreasing temperature. The current value of the mass flow rate is adapted to match the current decay power while keeping the temperature difference between steam inlet and water outlet constant at design conditions. Thus, the decay power equals the transferred power. The additional power for cool down of the water inventory is neglected because it only improves the behaviour of the system due to the higher power input. Furthermore, the additional power required for cool down depends on the water mass on the secondary side, which is not part of this analysis. Therefore, in the future the nuclear power plant model must be incorporated into the simulation. In Figure 8, the operation line of this simulation is shown. Similar to the previous simulation the operation condition moves towards the surge line. However, it stays in the stable region until the end of the simulation. The excess power of the system, shown in Figure 9 (top left), gradually reduces from 430 kW at full load to 40 kW at the end of the simulation. If the steam temperature is decreased further, or if the required power for other systems is too high, the power balance will become negative. Therefore, it can be concluded that the current design can be operated down to a part load of approximately 45 % in terms of thermal power. A better-optimized system might be able to reach even a lower load. To

follow the decay heat curve further, it would be necessary to switch off one system.

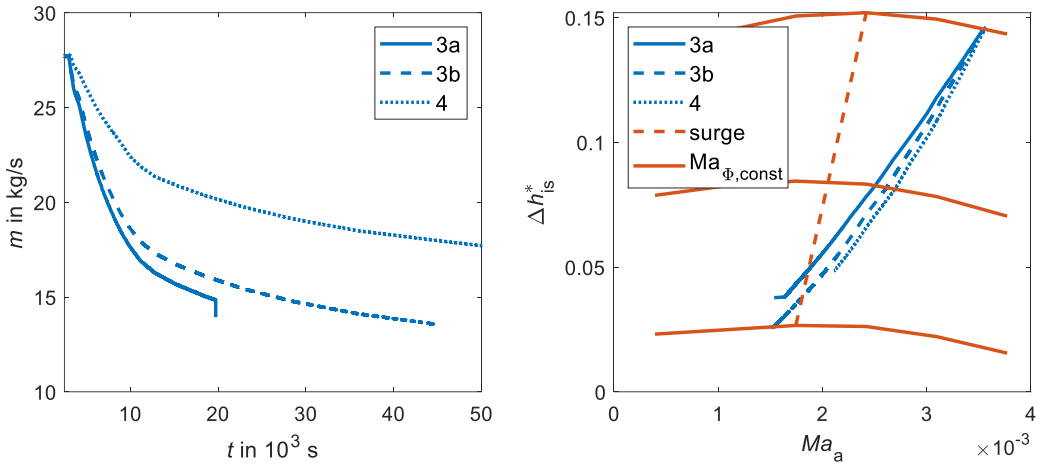

Figure 8: Compressor operation line on the dimensionless compressor map including the surge line (right) and mass flow rate of the sCO_2 cycle (left) for the simulations 3a, 3b and 4

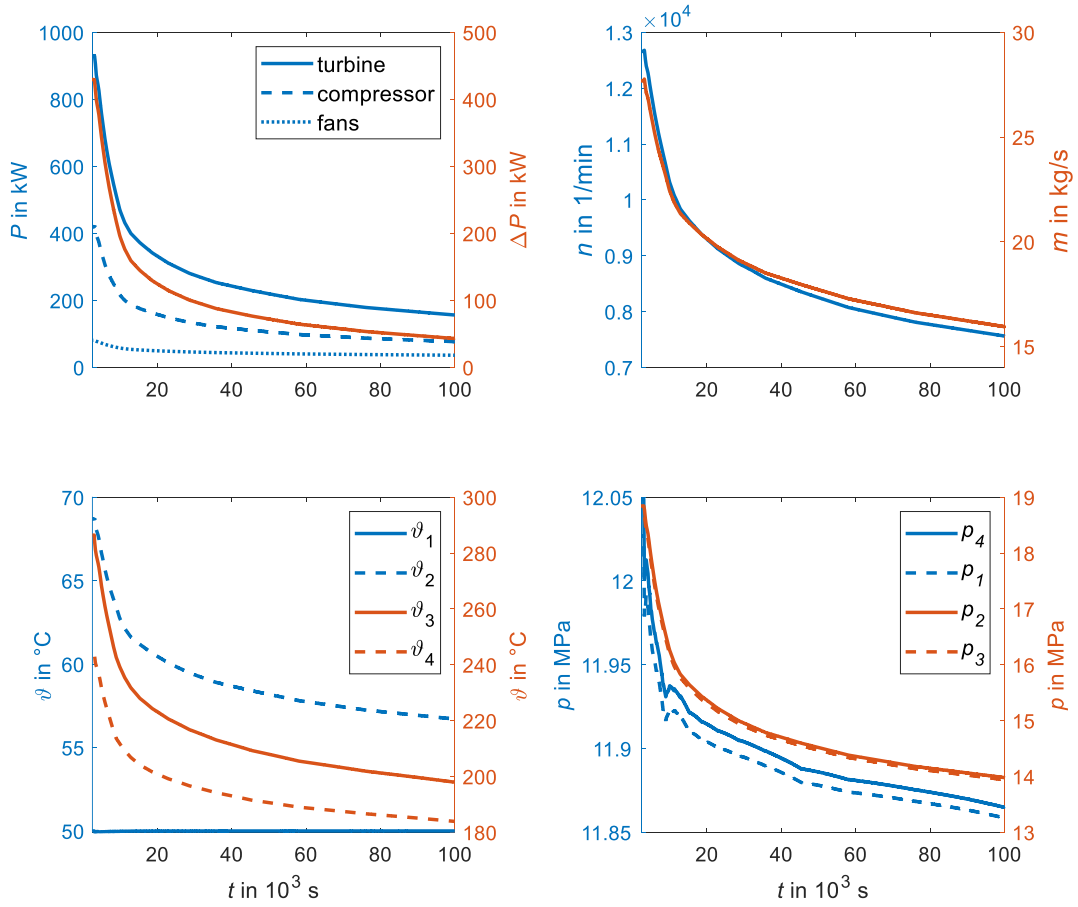

Figure 9: Power and excess power (top left), shaft speed and mass flow rate (top right), temperatures (bottom left) and pressures (bottom right) of simulation 4

In order to provide an overview of the successful simulation, the main results are summarized and displayed in Figure 9. At the end of the simulation, the speed of the turbomachinery is reduced to 60 % and the mass flow rate to 58 % (top right). The compressor inlet temperature ϑ_1 (bottom left) remains constant because it is controlled as proposed in the boundary conditions. The turbine inlet temperature ϑ_3 (bottom left) declines as a result of the declining steam temperature, which results in the intended decrease of the enthalpy difference over the CHX. The upper cycle pressures p_2 and p_3 (bottom right) are decreasing due to the decreasing pressure ratio of the compressor, which decreased from 1.57 at the design point to 1.18. The efficiencies of the turbomachinery stay close to their design values because the flow conditions inside the machines remained in a beneficial region. The non-smooth behaviour of the lower pressures p_1 and p_4 (bottom right) might be caused by the small change of the slope of the decay heat curve, which is input as table for this simulation. Furthermore, it must be noticed that p_1 and p_4 nearly stay constant, therefore small changes are clearly visible.

CONCLUSION

In this study, the sCO_2 heat removal system is designed and simulated under varying steam side boundary conditions. The simulations are carried out in the thermal-hydraulic system code ATHLET, which has been extended for the simulation of sCO_2 power cycles. The extensions include the thermodynamic properties, heat transfer and pressure drop correlations as well as performance map based turbomachinery models, which take the real gas behavior of sCO_2 into account.

The design of the sCO_2 cycle is conducted with a thermodynamic optimization maximizing the power output of the system. In order to extend the part load capability of the system, it might be beneficial to especially consider the part load operation of the turbomachinery together with the thermodynamic design in an integrated approach. Due to the application of an existing small-scale compressor map, the thermodynamic design point deviates from the optimal design point in terms of pressure ratio. However, this design with a relatively small pressure ratio of 1.57 was sufficient to ensure the operation of the system down to a part load of less than 50 % in terms of thermal power.

Two different failure modes of the system could be identified, namely a negative power balance and compressor surge. If the shaft speed of the cycle is not controlled, the cycle will remove more heat than is produced by the decay heat. This leads to a cool down of the steam side in the nuclear power plant and eventually stops the systems because the power balance becomes negative. To adapt to the declining decay heat curve, either single systems need to be switched off at the right time or the system must be controlled to remove less power from the nuclear power plant. The removed power can be adapted to the decay heat curve by controlling the shaft speed to keep the thermodynamic conditions at the steam side constant at design conditions. However, this drives the compressor to surge as the shaft speed is reduced. In order to avoid compressor surge, the steam side must be cooled down when the shaft speed is reduced.

In conclusion, instead of running the systems always at full speed also other operation strategies are possible. Considering all systems together, one operation strategy might be to follow the decay heat curve with all systems until the systems reach 50 % part-load. Then one system is switched off and the other systems are ramped up to a higher load again to compensate the loss of heat removal capacity. If the part load capability is 50 %, this procedure can be repeated until only one system is running, because when the second last system is shut down, the last system can be ramped up to 100 % again and compensates the loss of the second last system completely. If the operation point of the compressor moves too close to the surge line, the speed should not be reduced further. This causes a slow decline of the steam temperature since more power is removed than produced. Consequently, the operation point of the compressor moves away from the surge line and the speed can be reduced again. The advantage of this procedure is that, perhaps, this control strategy can be automatized and it is not necessary to determine the right time for the shutdown of single systems because in this strategy the shutdown condition of a single system is explicitly defined. Even if this strategy is not implemented in the beginning of the accident, it will be important in the long term when only one last system is still running.

The next step in the system analysis is to explicitly model the air-side of the UHS. Then it is possible to analyse the system behaviour and control under varying ambient temperatures. This enables to test strategies to avoid compressor surge at very low ambient temperatures. Afterwards, the condensation driven circulation loop on the steam side should be modelled and finally the whole nuclear power plant must be incorporated in the simulation to investigate the interaction of the sCO2-HeRo system with the nuclear power plant and other safety systems. In the future, the analysis will be conducted for a BWR as well as for a PWR to confirm and extend the knowledge basis for this new safety system. In parallel, the data and the models will be improved and validated further, e.g. the performance map of a large-scale compressor will be used and the turbomachinery and heat transfer models will be compared to experimental data.

NOMENCLATURE

c	speed of sound (m/s)
D	impeller diameter (m)
h	enthalpy (J/kg)
k_{fan}	relative power consumption of the fans (kW_{el} / MW_{th})
$\dot{m}$	mass flow rate (kg/s)
Ma_a	axial Mach number
Ma_θ	tangential Mach number
N	rotational speed (1/min)
p	pressure (MPa)
$\dot{Q}$	transferred power (W)
t	time (s)
x	steam quality
Greek letters	
Δh_{is}^*	dimensionless isentropic enthalpy difference
Δp	pressure drop (MPa)

ΔT_{PP}	pinch point temperature difference (K)
Δw	specific power output (J/kg)
ϑ	temperature (°C)
η_c	isentropic efficiency of compressor
η_t	isentropic efficiency of turbine
ρ	density (kg/m³)

Subscripts

1	compressor inlet
2	compressor outlet
3	turbine inlet
4	turbine outlet

Acronyms

ATHLET	Analysis of THermal-hydraulics of LEaks and Transients
BWR	boiling water reactor
CHX	compact heat exchanger
H_2O	water/steam
HeRo	heat removal system
PWR	pressurized water reactor
sCO_2	supercritical carbon dioxide
UHS	ultimate heat sink

ACKNOWLEDGEMENTS

The research presented in this paper has received funding from the Euratom research and training programme 2014-2018 under grant agreement No. 847606 “Innovative sCO2-based Heat removal Technology for an Increased Level of Safety of Nuclear Power plants” (sCO2-4-NPP).

The work of University of Stuttgart was also funded by the German Ministry for Economic Affairs and Energy (BMWi. Project No. 1501557) on basis of a decision by the German Bundestag.

REFERENCES

[1] Venker, J. (2015) Development and Validation of Models for Simulation of Supercritical Carbon Dioxide Brayton Cycles and Application to Self-Propelling Heat Removal Systems in Boiling Water Reactors. Stuttgart. https://doi.org/10.18419/opus-2364

[2] sCO2-HeRo. http://www.sco2-hero.eu/

[3] Benra, F.K., Brillert, D., Frybort, O., Hajer, P., Rohde, M., Schuster, S. et al. (2016) A supercritical CO2 low temperature Brayton-cycle for residual heat removal. *The 5th International Symposium-Supercritical CO2 Power Cycles*, 1–5. https://doi.org/10.1007/s13398-014-0173-7.2

[4] Bestion, D. (2008) System code models and capabilities. *THICKET*, Grenoble. p. 81–106.

[5] Mauger, G., Tauveron, N., Bentivoglio, F. and Ruby, A. (2019) On the dynamic modeling of Brayton cycle power conversion systems with the CATHARE-3 code. *Energy*, Elsevier Ltd. 168, 1002–16. https://doi.org/10.1016/j.energy.2018.11.063

[6] Batet, L., Alvarez-Fernandez, J.M., Mas de les Valls, E., Martinez-Quiroga, V., Perez, M., Reventos, F. et al. (2014) Modelling of a supercritical CO_2 power cycle for nuclear fusion reactors using RELAP5–3D. *Fusion Engineering and Design*, North-Holland. 89, 354–9. https://doi.org/10.1016/J.FUSENGDES.2014.03.018

[7] Hexemer, M.J., Hoang, H.T., Rahner, K.D., Siebert, B.W. and Wahl, G.D. (2009) Integrated Systems Test (IST) Brayton Loop Transient Model Description and Initial Results. *S-CO2 Power Cycle Symposium*, Troy. p. 1–172.

[8] Hofer, M., Buck, M. and Starflinger, J. (2019) ATHLET extensions for the simulation of supercritical carbon dioxide driven power cycles. *Kerntechnik*, 84, 390–6. https://doi.org/10.3139/124.190075

[9] IAEA. (1991) Safety related terms for advanced nuclear plants. Vienna.

[10] Hecker, F. and Seewald, M. (2018) Deliverable 4.2: BWR simulations of decay heat management. sCO2-HeRo.

[11] Hajek, P., Vojacek, A. and Hakl, V. (2018) Supercritical CO_2 Heat Removal System - Integration into the European PWR fleet. *2nd European SCO2 Conference*, Essen. p. 0–7. https://doi.org/10.17185/duepublico/460

[12] Vojacek, A., Hakl, V., Hajek, P., Havlin, J. and Zdenek, H. (2016) Deliverable 1.3: Documentation system integration into European PWR fleet. sCO2-HeRo.

[13] Hofer, M. and Starflinger, J. (2019) Preliminary analysis of the design and operation conditions of a sCO2 heat removal system. *Annual Meeting on Nuclear Technology*, Berlin. p. 1–8.

[14] Hacks, A.J., Vojacek, A., Dohmen, H.J. and Brillert, D. (2018) Experimental investigation of the sCO2-HeRo compressor. *2nd European SCO2 Conference 2018*, 0–10. https://doi.org/10.17185/duepublico/46088

[15] Lerchl, G., Austregesilo, H., Schöffel, P., von der Cron, D. and Weyermann, F. (2016) ATHLET User ’ s Manual. Garching. https://doi.org/10.1007/s00227-005-0161-8

[16] Straetz, M.R., Mertz, R. and Starflinger, J. (2018) Experimental investigation on the heat transfer between condensing steam and sCO2 in a compact heat exchanger. *2nd European SCO2 Conference 2018*,. https://doi.org/10.17185/DUEPUBLICO/46078

[17] Hofer, M., Buck, M., Strätz, M. and Starflinger, J. (2019) Investigation of a correlation based model for sCO2 compact heat exchangers. *3rd European Supercritical CO2 Conference*, Paris. p. 1–9. https://doi.org/10.17185/duepublico/48874

[18] Span, R. and Wagner, W. (1996) A new equation of state for carbon dioxide covering the fluid region from the triple-point temperature to 1100 K at pressures up to 800 MPa. *Journal of Physical and Chemical Reference Data*, 25, 1509–96. https://doi.org/10.1063/1.555991

[19] Hewitt, G.F. (1998) Heat exchanger design handbook. Begell House, New York.

[20] Dostal, V., Driscoll, M.J. and Hejzlar, P. (2004) A

Supercritical Carbon Dioxide Cycle for Next Generation Nuclear Reactors. *Technical Report MIT-ANP-TR-100*, 1–317. https://doi.org/MIT-ANP-TR-100

[21] Austregesilo, H., Bals, C., Hora, A., Lerchl, G., Romstedt, P., Schöffel, P. et al. (2016) ATHLET Models and Methods. Garching.

[22] Böckh, P. von and Wetzel, T. (2017) Wärmeübertragung: Grundlagen und Praxis. 7th ed. Springer, Berlin. https://doi.org/https://doi.org/10.1007/978-3-662-55480-7

[23] Numrich, R. and Müller, J. (2013) J1 Filmkondensation reiner Dämpfe. *VDI-Wärmeatlas*, Springer Berlin Heidelberg, Berlin, Heidelberg. p. 1011–28. https://doi.org/10.1007/978-3-642-19981-3_63

[24] Grote, W. (2009) Ein Beitrag zur modellbasierten Regelung von Entnahmedampfturbinen. Bochum.

[25] Dyreby, J.J., Klein, S.A., Nellis, G.F. and Reindl, D.T. (2012) Development of advanced off-design models for supercritical carbon dioxide power cycles. American Nuclear Society - ANS; La Grange Park (United States).

[26] Pham, H.S., Alpy, N., Ferrasse, J.H., Boutin, O., Tothill, M., Quenaut, J. et al. (2016) An approach for establishing the performance maps of the sc-CO2 compressor: Development and qualification by means of CFD simulations. *International Journal of Heat and Fluid Flow*, 61, 379–94. https://doi.org/10.1016/j.ijheatfluidflow.2016.05.017

[27] GEA Luftkühler GmbH. (2013) Luftgekühlter Wärmetauscher für CO2 (Angebot).

DOI: 10.17185/duepublico/73983
URN: urn:nbn:de:hbz:464-20210330-125241-0